ISSN 1674-1056
http://cpb.iphy.ac.cn
http://iopscience.iop.org/cpb
中国物理 B
Chinese Physics
中国物理
Chinese Physics B

How to characterize capacitance of organic optoelectronic devices accurately

Hao-Miao Yu(于浩淼), Yun He(何鋆)
Citation: Chin. Phys. B . 2018, 27(6): 067202. **doi:** 10.1088/1674-1056/27/6/067202

Journal homepage: http://cpb.iphy.ac.cn; http://iopscience.iop.org/cpb

What follows is a list of articles you may be interested in

First-principles hybrid functional study of the electronic structure and charge carrier mobility in perovskite $CH_3NH_3SnI_3$

Li-Juan Wu(伍丽娟), Yu-Qing Zhao(赵宇清), Chang-Wen Chen(陈畅文), Ling-Zhi Wang(王琳芝), Biao Liu(刘标), Meng-Qiu Cai(蔡孟秋)
Chin. Phys. B . 2016, 25(10): 107202. **doi:** 10.1088/1674-1056/25/10/107202

Alternating current characterization of nano-Pt(II) octaethylporphyrin (PtOEP) thin film as a new organic semiconductor

M Dongol, M M El-Nahass, A El-Denglawey, A A Abuelwafa, T Soga
Chin. Phys. B . 2016, 25(6): 067201. **doi:** 10.1088/1674-1056/25/6/067201

Effect of CuPc and MoO_3 co-evaporated layer on the conductivity of organic light emitting diodes

He Ze-Shang, Yu Hao-Miao, Peng Huan, Hou Xiao-Yuan
Chin. Phys. B . 2015, 24(9): 097201. **doi:** 10.1088/1674-1056/24/9/097201

Effect of traps'adjacency on the electric field dependence of mobility in organic systems

He Yun, Chen Xiao-Qing, Hou Xiao-Yuan
Chin. Phys. B . 2014, 23(9): 097201. **doi:** 10.1088/1674-1056/23/9/097201

Adsorption behavior of iron phthalocyanine on a Ag(110) surface

Wu Ke,Huang Qi-Huan,Zhang Han-Jie,Liao Qing,He Pi-Mo
Chin. Phys. B . 2012, 21(3): 037202. **doi:** 10.1088/1674-1056/21/3/037202

How to characterize capacitance of organic optoelectronic devices accurately*

Hao-Miao Yu(于浩淼)[1,†] and Yun He(何鋆)[2,‡]

[1] Key Laboratory of Luminescence and Optical Information, Ministry of Education, School of Science, Beijing Jiaotong University, Beijing 100044, China

[2] National Key Laboratory of Science and Technology on Space Microwave, China Academy of Space Technology (Xi'an), Xi'an 710100, China

(Received 26 December 2017; revised manuscript received 12 March 2018; published online 10 May 2018)

The selection of circuit model (i.e., parallel or series model) is critical when using a capacitance–frequency and capacitance–voltage technique to probe properties of organic materials and physical processes of organic optoelectronic devices. In the present work, capacitances of ITO/Alq_3/Al and ITO/CuPc/Al are characterized by series and parallel model, respectively. It is found that the large series resistance comes from the ITO electrode and results in the inapplicability of the parallel model to measuring the capacitances of organic devices at high frequencies. An equivalent circuit model with consideration of the parasitical inductance of cables is constructed to derive the capacitance, and actual capacitance–frequency spectra of Alq_3 and CuPc devices are obtained. Further investigation of temperature-dependent capacitance–frequency and capacitance–voltage characteristics indicates that CuPc and Al form the Schottky contact, the density and ionization energy of impurities in CuPc are obtained. Moreover, more practical guidelines for accurate capacitance measurement are introduced instead of the impedance magnitude, which will be very helpful for the organic community to investigate capacitance-related characteristics when dealing with various organic optoelectronic devices.

Keywords: organic semiconductor, capacitance characterization, Schottky contact, ionization energy

PACS: 72.20.Jv, 72.80.Le, 73.30.+y, 73.61.Ph **DOI:** 10.1088/1674-1056/27/6/067202

1. Introduction

In the field of organic semiconductors, capacitance–frequency (C–F), and capacitance–voltage (C–V) methods are widely used to study their properties, including doping density,[1–4] deep trap states,[5–7] carrier mobility,[8–10] etc. A common issue in these studies is the selection of a circuit model (i.e., parallel or series model), which is critical to the accurate determination of the device capacitance. Figure 1(a) shows the small-signal equivalent circuit for capacitance measurement. In this figure R_{p0} represents the parallel resistance, R_{s0} the series resistance, and C the capacitance, and R_{p0} is expected to be quite large and R_{s0} quite small for most capacitive devices. When performing the measurement, the LCR meter basically measures the module and phase of impedance via LCR bridges, and then they are calculated by using the corresponding parameters according to the model selected. As the information contained in impedance (real and imaginary parts) can be transformed into two equations only, thus their solution contains neither more nor less than two parameters, i.e., the circuit model should comprise two elements only, this is why the approximate model has to be chosen instead of the model shown in Fig. 1(a). For the frequencies at which R_{s0} is negligible compared with large capacitive impedance, the parallel model shown in Fig. 1(b) is a good approximation of the equivalent circuit, where R_p and C_p represent the parallel resistance and the capacitance, respectively. While for the frequencies at which R_{s0} is comparable to capacitive impedance, it is an un-negligible voltage divider, in such a case the series model shown in Fig. 1(c) is the most accurate approximation, where R_s and C_s represent the series resistance and the capacitance, respectively. In the field of inorganic semiconductors, a parallel model is used to investigate the capacitance properties of devices, as the series resistance is negligible compared with capacitive impedance in the frequency range of interest (10 Hz–1 MHz), and this model is directly adopted by the organic community.[7,9,10] Few researches have examined the validity of employing a parallel model to measure the capacitance of organic optoelectronic devices except Carr's report;[11] they pointed out that the impedance magnitude should be monitored and correspondingly employed an appropriate model. In brief, the parallel model should be selected within lower frequencies, and the series model within higher ones due to the large series resistance. Though their analysis and suggestions are reasonable, they are not completely convincing without ascertaining the origin of series resistance, and corresponding researches are lacking so far. Besides, some reports have mentioned that resonance appears in the C–F spectrum and prevent the analysis at high frequencies (usually above 100 kHz).[7] To further study and elucidate these issues, two types of organic materials, CuPc and Alq_3, which are commonly used in organic optoelectronic devices

*Project supported by the Fundamental Research Funds for the Central Universities, China

†Corresponding author. E-mail: yuhaomiao@bjtu.edu.cn

‡Corresponding author. E-mail: 081019028@fudan.edu.cn

© 2018 Chinese Physical Society and IOP Publishing Ltd

are employed and their distinct C–F and C–V characteristics are investigated in the present work.[12–15] The origin of large series resistance is confirmed, moreover, general guidelines for model selection and accurate capacitance measurement of organic devices are introduced, especially for those with ITO electrodes.

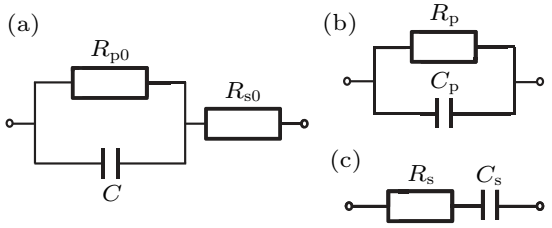


Fig. 1. (a) Small-signal equivalent circuit. (b) Parallel approximation of equivalent circuit (parallel model). (c) Series approximation of equivalent circuit (series model).

2. Experimental methods

In the present study, all the devices were fabricated using the method described elsewhere.[16] Commercial materials Alq_3 and CuPc with purity $> 99\%$ were used without further purification. Capacitance properties of the devices were measured with a programmed HP 4284A LCR Meter. A parallel model was chosen to measure the C–V characteristics of devices; the ITO side was positively biased with respect to the Al side and the corresponding frequency of AC bias modulation was 1 kHz. Excepting C–V measurement, all impedance measurements were performed without external bias voltage. During the measurement, devices with structure of ITO/organic/Al and effective size of 4 mm×4 mm were placed in a dark liquid nitrogen Dewar bottle with a temperature controller; the temperature was 297 K unless otherwise specified.

3. Results and discussion

Firstly, series and parallel models are used to measure the C–F characteristics of ITO/Alq_3 (200 nm)/Al and ITO/CuPc (310 nm)/Al, and the results are shown in Fig. 2. For the Alq_3 device, C_p keeps almost unchanged at frequencies in a range of 40 Hz–30 kHz, and it turns to decrease rapidly with increasing frequency in a range of 30 kHz–1 MHz. But C_s keeps unchanged in a wider frequency range of 40 Hz–300 kHz, and it increases slowly with increasing frequency in a range of 300 kHz–1 MHz. For the CuPc device, C_p decreases slowly with increasing frequency in a range of 40 Hz–10 kHz, and it turns to decrease rapidly with increasing frequency in a range of 10 kHz–1 MHz, while C_s decreases slowly with increasing frequency in a range of 40 Hz–600 kHz, and it turns to increase with increasing frequency in a range of 600 kHz–1 MHz. At low frequencies, C_s and C_p are equal for each device, and the capacitance of the Alq_3 device exhibits a flat frequency response, which indicates that the ITO/Alq_3/Al device is an ideal parallel plate capacitor. However, at high frequencies, the difference between C_s and C_p is apparent for each device, the higher the frequency, the bigger the difference is. As illustrated by the equivalent circuit in Fig. 1(a), at low frequencies, capacitive impedance is much larger than R_{s0} and R_{p0} is expected to be quite large, thus R_{s0} is negligible and capacitive impedance dominates the impedance of the circuit. As the capacitive impedance decreases with increasing frequency, it fails to dominate the characteristics of the circuit impedance when it is comparable to R_{s0}, and the parallel model is no longer an accurate approximation as R_{s0} is not negligible. Thus an apparent difference between C_s and C_p is observed. With frequency further increasing, capacitive impedance becomes negligible compared with R_{s0} and R_{s0} will dominate circuit impedance, the impedance will exhibit a flat frequency response. The capacitance reveals the intrinsic nature of the material or device, and it should not vary with model selection, but the fact is not so, thus the applicabilities of two models should be examined.

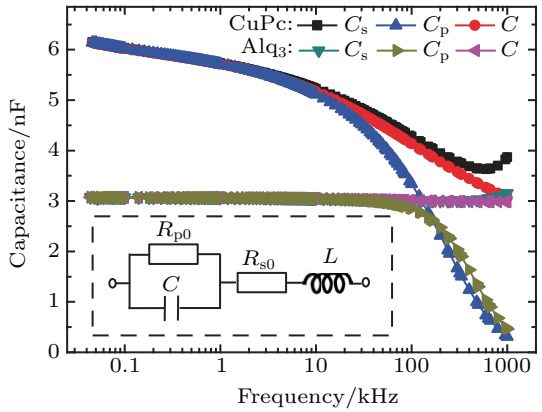


Fig. 2. (color online) Curves of C–F characteristics versus frequency of ITO/Alq_3 (200 nm)/Al and ITO/CuPc (310 nm)/Al, with C_p and C_s being the capacitances measured under parallel and series model, respectively. Inset shows the equivalent circuit model with consideration of parasitical inductance of cables, and C is calculated from data measured under parallel model according to Eq. (1).

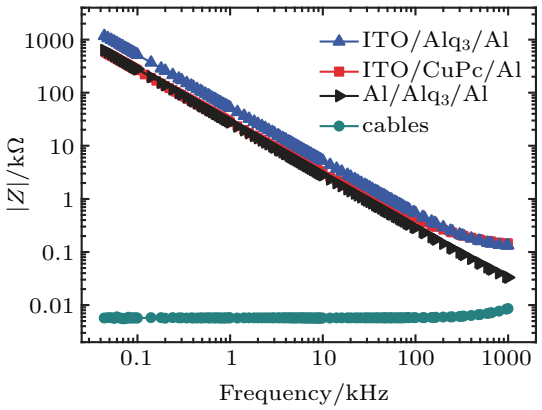


Fig. 3. (color online) Plots of Z–F characteristics of ITO/Alq_3 (200 nm)/Al, Al/Alq_3 (110 nm)/Al, ITO/CuPc (310 nm)/Al, and cables.

For further investigation, the impedance–frequency (Z–F) characteristics of two devices are measured and shown in Fig. 3 with coordinate axes being logarithmically scaled. As

shown in Fig. 3, for both devices, the impedance decreases linearly with frequency in a range of 40 Hz–100 kHz, and it continues to decrease with frequency but deviates from linearity in a range of 100 kHz–1 MHz, the higher the frequency, the more slowly the impedance decreases with frequency in this region. It almost does not change when frequency approaches to 1 MHz, and the corresponding value is about 132 Ω. Notice that the impedance values of two different devices approach nearly to the same value at 1 MHz. The slopes of linear fitting of $\log|Z| - \log F$ in a range of 40 Hz–100 kHz are about -0.99 and -0.94 for Alq_3 and CuPc devices, respectively, in accordance with the characteristic of capacitive impedance, i.e., $|Z| \propto 1/F$, which indicates that devices are capacitive. When frequency approaches to 1 MHz, the frequency-independent impedance strongly indicates that a resistance exists. According to the circuit shown in Fig. 1(a), this resistance is just the R_{s0}, and its value is 132 Ω. The two electrodes of the device are ITO and Al, respectively, but the resistances of the Al electrode and cables are quite small: they are negligible compared with high R_{s0} of 132 Ω, thus it (i.e., impedance at high frequencies) must come from ITO. To confirm this, the device with a structure of Al/Alq_3/Al is fabricated, its Z–F relationship along with that of cables are also shown in Fig. 3. The impedance of the Alq_3 device decreases linearly with increasing frequency in the whole frequency range with substitution of Al for ITO, which indicates that the large R_{s0} indeed comes from ITO. The impedance of cables does not change with frequency in a range of 40 Hz–300 kHz and its value is about 5.7 Ω, while it begins to increase with increasing frequency in a range of 300 kHz–1 MHz; this means that the parasitical inductance of cables takes effect at high frequencies. The Z–F characteristic of cables indicates that the resistance of cables which contributes to series resistance is about 5.7 Ω; once the frequency exceeds 300 kHz, parasitical inductance begins to affect the characteristic of impedance. As shown in Fig. 3, at higher frequencies the impedance of cables is comparable to that of the Al/Alq_3/Al device, thus the influence of the parasitical inductance of cables cannot be neglected.

Taking the parasitical inductance of cables into account, a new equivalent circuit model without approximation is established and shown in Fig. 2 (the inset). As R_{s0} and parasitical inductance can be measured or calculated from the Z–F relationship at high frequencies, the actual capacitance can be directly calculated from the data measured under the parallel model according to

$$C = \frac{L + C_p R_p^2 + C_p^2 R_p^2 L\omega^2}{-2R_p R_{s0} + R_{s0}^2 + L^2\omega^2 + R_p^2[1 + 2C_p L\omega^2 + C_p^2\omega^2(R_{s0}^2 + L^2\omega^2)]}, \tag{1}$$

where L is the parasitical inductance and ω is the angular frequency. The capacitance of ITO/Alq_3 (200 nm)/Al and ITO/CuPc (310 nm)/Al calculated according to Eq. (1) is shown in Fig. 2. The capacitance of the Alq_3 device exhibits almost a flat frequency, while that of the CuPc device decreases with frequency in a range of 40 Hz–1 MHz. Note that the influence of cables can be eliminated by performing open-short compensation,[17] in such a case its resistance contributing to series resistance and parasitical inductance (L in the inset of Fig. 2) are both zero, and the series model will be an appropriate approximation at high frequencies.

The C–F characteristics of Alq_3 and CuPc devices are quite different. The capacitance of the Alq_3 device exhibits almost a flat frequency, which is a typical characteristic of a capacitor and means that Alq_3 is an ideal insulating dielectric. For the CuPc device, however, its capacitance is frequency dependent; this phenomenon has been reported in many reports about inorganic and organic semiconductors, and it is related to the temperature-dependent properties of impurities or defects.[18–21] Thus the C–F characterizations of the CuPc device are carried out at different temperatures and the results are shown in Fig. 4. Each capacitance decreases with increasing frequency in the range of 40 Hz–1 MHz for the temperatures above 79 K. However, it almost does not change with frequency at a temperature of 79 K. The higher the temperature, the larger the variation with frequency will be, e.g., the capacitance decreases from 6.14 nF to 3.06 nF as frequency increases from 40 Hz to 1 MHz, which is nearly a half reduction. The capacitance at low frequency increases a lot as temperature increases due to the enhanced thermally activated free carriers. But at high frequencies, free charge carriers cannot respond, and the capacitance begins to decrease quickly, so the rate of reduction of capacitance becomes larger as temperature increases. The capacitance also shows strong temperature dependence, e.g., it increases from 2.54 nF to 6.02 nF as temperature increases from 79 K to 297 K at frequency 100 Hz, which is about a 137% increase. The frequency dispersion of capacitance can be explained by the hole emission and capture process of impurities, which is characterized by the ionization time and it decreases with temperature increasing.[18–21] When the process is able to keep up with the variation of AC bias modulation, i.e., the ionization time is much shorter than the period of the AC modulation signal, the capacitance does not change in a certain frequency range. But when the frequency is beyond that range it will not be able to respond to the AC signal timely, resulting in the capacitance decreasing with frequency increasing. With frequency further increasing, it will not respond to modulation and capacitance will not change

with frequency.

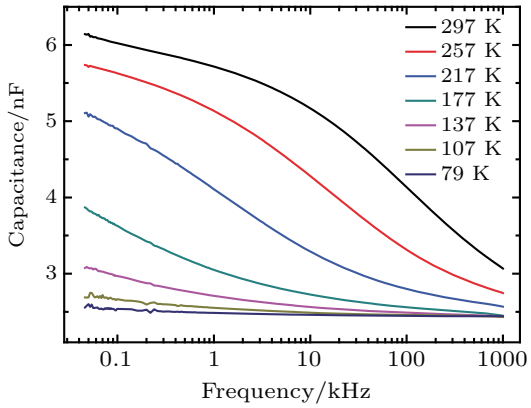


Fig. 4. (color online) Curves of capacitance versus frequency of ITO/CuPc(310 nm)/Al at different temperatures. The capacitance is calculated from Eq. (1).

Figure 4 shows that when temperature decreases to 79 K, the frequency dispersion of the capacitance of the CuPc device almost disappears, just like that of the Alq_3 device measured at room temperature. That means that the emission and capture process of holes can hardly keep up with the variation of AC bias modulation in the whole frequency region. The process cannot respond to the frequency as low as 40 Hz; it is more probable that impurities are hardly ionized. A simple way to confirm or exclude this possibility is to investigate the C–V characteristics of the device. Figure 5 shows the C–V characteristics of CuPc and Alq_3 devices. The capacitance of the CuPc device increases with voltage when temperature is at 297 K, while it does not change with voltage when temperature decreases to 79 K. For the Alq_3 device, capacitance does not change with voltage even at 297 K. As is well known, if the metal and inorganic semiconductor form a Schottky contact, there will be a space charge region in the semiconductor. The barrier capacitance and bias applied satisfy the relationship:[22]

$$\frac{1}{C^2} = 2\frac{V_{\rm d} - V}{A^2 e\varepsilon_0 \varepsilon N}, \tag{2}$$

where $V_{\rm d}$ is the difference between the work function of the metal and Femi level of the semiconductor divided by e (the elementary charge), V is the bias applied, A is the area, ε is the relative dielectric constant of the semiconductor, ε_0 is the dielectric constant of the vacuum, and N is the density of space charge (equal to the density of ionized dopants under depletion approximation) in the semiconductor. The inset of Fig. 5 shows that the relationship between $1/C^2$ and V is linear, in accordance with Eq. (2). This strongly indicates the formation of a Schottky contact between CuPc and Al, as indicated in many reports the ITO-CuPc contact is Ohmic.[23,24] The density of impurities and $V_{\rm d}$ can be obtained by the linear fitting of $1/C^2$–V along with Eq. (1), they are about 3.1×10^{16} cm^{-3} and 0.88 V, respectively. For the CuPc device at 79 K and the Alq_3 device at 297 K, neither of their capacitances changes with bias, which indicates a case of flat-band, i.e., no space charge region existing in the organic layer. As temperature decreases from 297 K to 79 K, the space charge region in the CuPc layer disappears, this means that there are none of the ionized impurities, i.e., there are no free carriers existing in CuPc, and it is an insulating dielectric at 79 K.

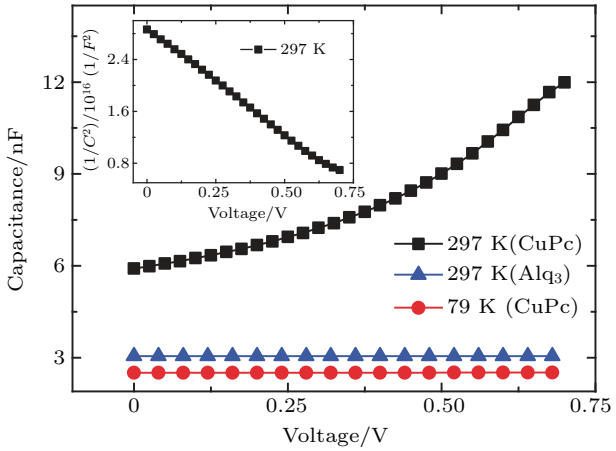


Fig. 5. (color online) Curves of C–V characteristics of ITO/CuPc (310 nm)/Al and ITO/Alq_3 (200 nm)/Al, with the inset showing the relationship between the reciprocal of the square of the capacitance and the bias applied to the CuPc device.

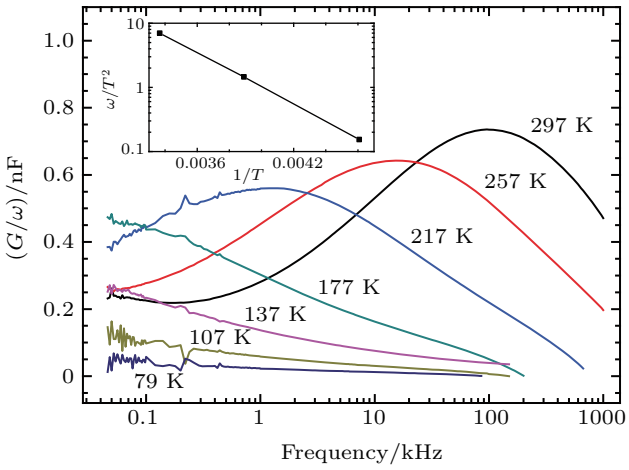


Fig. 6. (color online) Plots of G/ω versus frequency at different temperatures, here G equals the reciprocal of $R_{\rm p0}$ shown in the inset of Fig. 2. The inset shows the relationship between peak frequency and temperature, i.e., $\ln(\omega/T^2)$ versus $1/T$.

According to previous reports about inorganic Schottky diodes, the ionization energy of impurities could be obtained by analyzing the temperature-dependent C–F or G/ω–F characteristics,[18,19] here, G is the conductance and ω is the angular frequency. When the ionization time is equal to the period of AC signal the conductance will reach a peak. Figure 6 shows G/ω–F characteristics of the CuPc device. For each of the curves above 177 K, the value of G/ω first increases with frequency and reaches its own maximum value, then deceases with frequency increasing, and the peak frequency increases with temperature rising. For each of the curves below 177 K, the value of G/ω decreases with frequency increasing. An Arrhenius plot of $\ln(\omega/T^2)$ versus $1/T$ should yield

a straight line and its slope is equal to ionization energy E_D divided by Boltzmann constant k, here, ω corresponds to the peak frequency.[19,20] The inset of Fig. 6 indicates a linear relationship between $\ln(\omega/T^2)$ and $1/T$, and the fitted ionization energy E_D is about 0.26 eV.

The parallel model is widely adopted to measure the capacitance of the organic optoelectronic device,[7,9,10] however, Carr *et al*., indicated that it cannot be indiscriminately used in a frequency range of interest, and a hybrid model should be used according to the impedance magnitude (parallel model within lower frequencies and series model within higher ones) instead.[11] In the present work, it is found that large series resistance comes from the ITO electrode by analyzing the *Z*–*F* relationship and results in the inapplicability of the parallel model to measure capacitance at high frequencies, thus special attention should be paid to model selection when characterizing the capacitance of an organic device with an ITO electrode. Moreover, it is demonstrated that it is essential to investigate the *Z*–*F* characteristics to select the circuit model and determine the capacitance accurately. For various organic devices, their capacitances and series resistances vary with many factors, such as the kind of electrode, thickness of organic layer, and effective area; using the impedance magnitude as a guideline of model selection is too simple as it will not give information about which part of the circuit dominates the impedance. The *Z*–*F* relationship, however, will explicitly reveal the dominating factors over the frequency range of interest as shown in the present work, thus it will give better guidelines for model selection than the impedance magnitude. During the measurement of capacitance, the influence of cables especially its parasitical inductance cannot be ignored. As shown in the present work, the parasitical inductance of the cables which can be eliminated by performing open-short compensation accounts for the series model failing to measure the capacitance at high frequency, and it may be the cause of resonance appearing in the capacitance spectrum in the high frequency region (usually above 100 kHz), which has been mentioned in some reports.[7] Besides, the capacitance of an organic device can be accurately calculated from the data measured under the parallel model according to Eq. (1) without any approximation, if series resistance can be measured at high frequencies.

The *C*–*V* and *C*–*F* characteristics of the CuPc device indicate that there are thermally activated free carriers existing in CuPc. For Alq_3, however, there are no free carriers existing even at room temperature. Though the purity of commercial material CuPc is $> 99\%$, the remaining chemical impurities could be ionized at high temperatures, and thus providing free carriers. Another possible origin of these free carriers is the defect states. Thermally evaporated CuPc layer with highly structural disorder may result in some defect state, and such a defect state could be activated thermally and provide free carriers at high temperatures. More studies are needed to further ascertain the origin of free carriers in CuPc.

4. Conclusions

In this work, series and parallel models are used to characterize the capacitances of ITO/Alq_3/Al and ITO/CuPc/Al. It is found that the large series resistance of the device comes from the ITO electrode and results in the inapplicability of the parallel model to measuring the capacitance of the organic device at high frequencies, its value is obtained by analyzing the *Z*–*F* relationship. An equivalent circuit model with consideration of the parasitical inductance of cables is constructed to characterize the capacitance of the device accurately, and *C*–*F* spectra of Alq_3 and CuPc devices are obtained. The further investigation of temperature-dependent *C*–*F* and *C*–*V* characteristics indicates that CuPc and Al form the Schottky contact, and the density and ionization energy of impurities are also obtained.

Acknowledgment

The authors thank Prof. Xiaoyuan Hou for his useful suggestion.

References

[1] Tomozawa H, Braun D, Phillips S, Heeger A J and Kroemer H 1987 *Synth. Met.* **22** 63
[2] Sharma G D, Saxena Dhiraj and Roy M S 2001 *Synth. Met.* **123** 189
[3] Dennler G, Lungenschmied C, Sariciftci N S, Schwödiauer R, Bauer S and Reiss H 2005 *Appl. Phys. Lett.* **87** 163501
[4] Guvenc Ali Bilge, Yengel Emre, Wang Guoping, Ozkan Cengiz S and Ozkan Mihrimah 2010 *Appl. Phys. Lett.* **96** 143301
[5] Sharma A, Kumar P, Singh B, Chaudhuri S R and Ghosh S 2011 *Appl. Phys. Lett.* **99** 023301
[6] Boix Pablo P, Garcia-Belmonte Germà, Muñecas Udane, Neophytou Marios, Waldauf Christoph and Pacios Roberto 2009 *Appl. Phys. Lett.* **95** 233302
[7] Reis F T, Mencaraglia D, Saad S Oould, Séguy I, Oukachmih M, Jolinat P and Destruel P 2003 *Synth. Met.* **138** 33
[8] Li Jian V, Nardes Alexandre M, Liang Ziqi, Shaheen Sean E, Gregg Brian A and Levi Dean H 2011 *Org. Electron.* **12** 1879
[9] Gommans H H P, Kemerink M, Andersson G G and Pijper R M T 2004 *Phys. Rev. B* **69** 155216
[10] Tsang S W, So S K and Xu J B 2006 *J. Appl. Phys.* **99** 013706
[11] Carr J A and Chaudhary S 2012 *Appl. Phys. Lett.* **100** 213902
[12] Vestweber H and Riess W 1997 *Synth. Met.* **91** 181
[13] Liu Z T, Lo M F, Wang H B, Ng T W, Roy V A L, Lee C S and Lee S T 2009 *Appl. Phys. Lett.* **95** 093307
[14] Ai Yuming, Gowrisanker Srinivas, Jia Huiping, Trachtenberg Isaac, Vogel Eric, Wallace Robert M, Gnade Bruce E, Barnett Raymond, Stiegler Harvey and Edwards Hal 2007 *Appl. Phys. Lett.* **90** 262105
[15] Song Q L, Li C M, Chan-Park Mary B, Lu M, Yang H and Hou X Y 2007 *Phys. Rev. Lett.* **98** 176403
[16] He Y, Hu Y M, Chen X Q, Peng H, You Y T, Zeng Q, Gao X D and Hou X Y 2013 *J. Phys. Chem. C* **117** 9143
[17] Agilent Technologies 2009 *Agilent Impedance Measurement Handbook*, 4th edn.
[18] Vincent G, Bois D and Pinard P 1975 *J. Appl. Phys.* **46** 5173
[19] Koide Y, Koizumi S, Kanda H, Suzuki M, Yoshida H, Sakuma N, Ono T and Sakai T 2005 *Appl. Phys. Lett.* **86** 232105
[20] Los A V and Mazzola M S 2001 *J. Appl. Phys.* **89** 3999
[21] Los A V and Mazzola M S 2001 *J. Electron. Mater.* **30** 235
[22] Sze S M and Ng Kwok K 2006 *Physics of Semiconductor Devices*, 3rd edn. (John Wiley & Sons)
[23] Mahapatro Ajit Kumar and Ghosh Subhasis 2002 *Appl. Phys. Lett.* **80** 4840
[24] Kwong C Y, Djurišiĉ A B, Chui P C, Lam L S M and Chan W K 2003 *Appl. Phys. A-Mater. Sci. Process.* **77** 555